Human B cell clonal expansion and convergent antibody responses to SARS-CoV-2

Authors: Sandra C. A. Nielsen[1,12], Fan Yang[1,12], Katherine J. L. Jackson[2,12], Ramona A. Hoh[1,12], Katharina Röltgen[1], Bryan Stevens[1], Ji-Yeun Lee[1], Arjun Rustagi[3], Angela J. Rogers[4], Abigail E. Powell[5], Javaria Najeeb[6], Ana R. Otrelo-Cardoso[6], Kathryn E. Yost[7], Bence Daniel[1], Howard Y. Chang[7,8], Ansuman T. Satpathy[1], Theodore S. Jardetzky[6,9], Peter S. Kim[5,10], Taia T. Wang[3,10,11], Benjamin A. Pinsky[1], Catherine A. Blish[3,10*], Scott D. Boyd[1,9,13*]

Affiliations:

[1]Department of Pathology, Stanford University, Stanford, CA 94305, USA.

[2]Garvan Institute of Medical Research, Darlinghurst, NSW 2010, Australia.

[3]Department of Medicine, Division of Infectious Diseases and Geographic Medicine, Stanford University, Stanford, CA 94305, USA.

[4]Department of Medicine, Division of Pulmonary, Allergy and Critical Care Medicine, Stanford University, Stanford, CA 94305, USA.

[5]Stanford ChEM-H and Department of Biochemistry, Stanford University, Stanford, CA 94305, USA.

[6]Department of Structural Biology, Stanford University, Stanford, CA 94305, USA.

[7]Center for Personal Dynamic Regulomes, Stanford University, Stanford, CA 94305, USA.

[8]Howard Hughes Medical Institute, Stanford University, Stanford, CA 94305, USA.

[9]Sean N. Parker Center for Allergy and Asthma Research, Stanford, CA 94305, USA.

[10]Chan Zuckerberg Biohub, San Francisco, CA 94158, USA.

22   [11]Department of Microbiology and Immunology, Stanford University, Stanford, CA 94305,

23   USA.

24   [12]These authors contributed equally

25   [13]Lead Contact

26   [*]Correspondence: cblish@stanford.edu (C.A.B.), sboyd1@stanford.edu (S.D.B.)

27

SUMMARY

29   During virus infection B cells are critical for the production of antibodies and protective

30   immunity. Here we show that the human B cell compartment in patients with diagnostically

31   confirmed SARS-CoV-2 and clinical COVID-19 is rapidly altered with the early recruitment of

32   B cells expressing a limited subset of IGHV genes, progressing to a highly polyclonal response

33   of B cells with broader IGHV gene usage and extensive class switching to IgG and IgA

34   subclasses with limited somatic hypermutation in the initial weeks of infection. We identify

35   extensive convergence of antibody sequences across SARS-CoV-2 patients, highlighting

36   stereotyped naïve responses to this virus. Notably, sequence-based detection in COVID-19

37   patients of convergent B cell clonotypes previously reported in SARS-CoV infection predicts the

38   presence of SARS-CoV/SARS-CoV-2 cross-reactive antibody titers specific for the receptor-

39   binding domain. These findings offer molecular insights into shared features of human B cell

40   responses to SARS-CoV-2 and other zoonotic spillover coronaviruses.

41

KEYWORDS

43   COVID-19, SARS-CoV-2, B cells, clonal expansion, antibodies, immunogenetics, convergent

44   antibody response, primary infection, immunology, antibody repertoire.

45

46   **INTRODUCTION**

47   The novel human severe acute respiratory syndrome coronavirus 2 (SARS-CoV-2) is the

48   etiological agent of the coronavirus disease 2019 (COVID-19) (Huang et al., 2020; Zhu et al.,

49   2020) pandemic. Prior to the emergence of SARS-CoV-2, six human coronaviruses (hCoVs)

50   were known; four seasonal hCoVs (hCoV-229E, -NL63, -HKU1, and -OC43) (Su et al., 2016)

51   causing usually mild upper respiratory illness, and the two more recently discovered SARS-CoV

52   (Peiris et al., 2003) and MERS-CoV (Zaki et al., 2012) viruses that arose from spillover events of

53   virus from animals into humans. It is expected that humans are naïve to SARS-CoV-2 and will

54   display a primary immune response to infection. Humoral immune responses will likely be

55   critical for the development of protective immunity to SARS-CoV-2. Recently, many novel

56   SARS-CoV-2 neutralizing antibodies from convalescent COVID-19 patients have been reported

57   (Cao et al., 2020; Ju et al., 2020; Robbiani et al., 2020b; Wu et al., 2020b), which offer an

58   important resource to identify potential protective or therapeutic antibodies. However, a deeper

59   understanding of the B cell antigen receptors that are stimulated and specific to this acute

60   infection is needed to define the shared or distinct features of humoral responses elicited

61   compared to other viral infections, and to assess the extent to which responses to SARS-CoV-2

62   have breadth extending to other coronaviruses within the subgenus Sarbecovirus.

63

64   **RESULTS**

65   **SARS-CoV-2 infection causes global changes in the antibody repertoire**

66   High-throughput DNA sequencing of B cell receptor heavy chain genes defines clonal B cell

67   lineages based on their unique receptor sequences, and captures the hallmarks of clonal

3

68   evolution, such as somatic hypermutation (SHM) and class switch recombination during the

69   evolving humoral response (Zhou and Kleinstein, 2019). To study the development of SARS-

70   CoV-2-specific humoral responses, we collected a total of 38 longitudinal peripheral blood

71   specimens from 13 patients, sampled at a median of 3 time points (range 1-5) admitted to

72   Stanford Hospital with COVID-19 confirmed by quantitative reverse transcription PCR (RT-

73   qPCR) testing. The times of blood sampling were measured as days post symptom onset

74   (DPSO). All patients exhibited SARS-CoV-2 receptor-binding domain (RBD)-specific IgA, IgG,

75   and IgM antibodies (Table 1). Immunoglobulin heavy chain (IGH) repertoires were sequenced

76   and compared to a healthy human control (HHC) data set from 114 individuals (Nielsen et al.,

77   2019). An example of data from a HHC individual matched by mean sequencing depth of reads

78   and B cell clones across the COVID-19 cohort is shown in Figure 1 (top panel). In healthy

79   subjects at baseline, IgM and IgD sequences are primarily derived from naïve B cells with

80   unmutated IGHV genes, whereas class switched cells expressing IgA or IgG subtypes have

81   elevated SHM. In contrast, SARS-CoV-2 seroconverted patients (blue labels in Figure 1), show a

82   highly polyclonal burst of B cell clones expressing IgG, and to a lesser extent IgA, with little to

83   no SHM. Longitudinal data from a patient prior to and after seroconversion shows an increase in

84   the proportion of class switched low SHM clones (bottom panels in Figure 1). Seronegative

85   samples (red labels in Figure 1) show IGH repertoires similar to uninfected HHC, suggesting an

86   earlier stage in the infection for these particular patients at these time points.
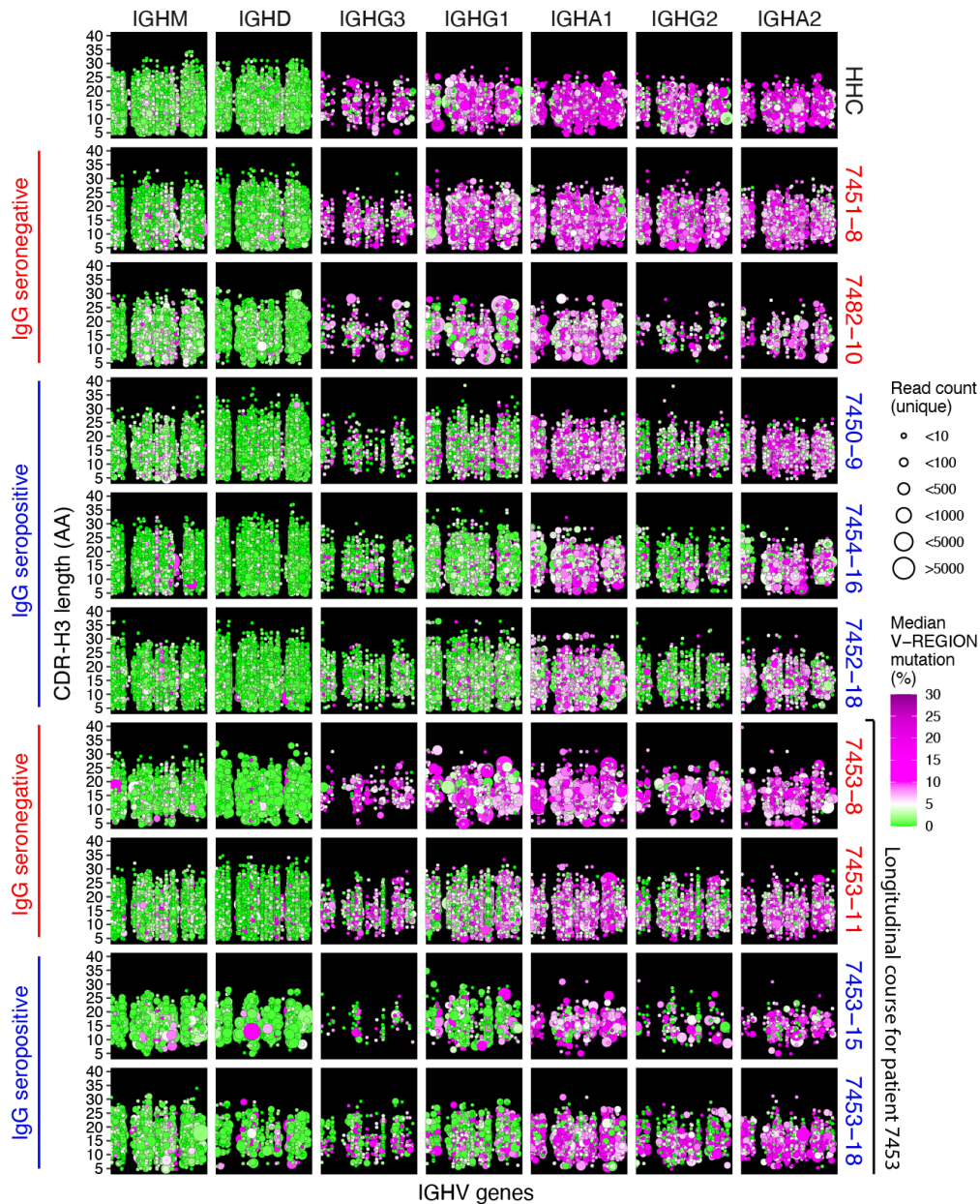
Figure 1. COVID-19 patient IGH repertoires show early and extensive class-switching to IgG and IgA subclasses without significant somatic mutation. Points indicate B cell clonal lineages, with the position denoting the clone's isotype (panel column), human healthy control (HHC) or patient ID (panel row), IGHV gene (x-axis, with IGHV gene in the same order and position in panels, but not listed by name due to space constraints), and CDR-H3 length in amino acids (AA) (y-axis within each panel). The point color indicates the median IGHV SHM frequency for each clone and the size indicates the number of unique reads grouped into the clone. Points are jittered to decrease over-plotting of clones with same IGHV gene and CDR-H3 length. Patient label colors indicate sample IgG seroconversion (blue) or seronegative (red) for the displayed sample with the number following the patient ID corresponding to days post symptom onset. The final four rows of panels show the IGH repertoire changes within a single participant (7453) prior to and after seroconversion.

5

99   The increased fraction of unmutated and low mutation (<1% SHM in IGHV gene) clones among

100   the class switched IgG subclasses in seroconverted COVID-19 patients compared to HHC was

101   statistically significant (IgG1: p-value = 1.884e-08; IgG2: 1.554e-08; IgG3: 3.754e-08; IgG4:

102   0.00044) (Figures 2A and 2B). The detailed SHM frequencies and fractions of unmutated clones

103   of each sample are shown in Figure S1. While most B cells in COVID-19 patients prior to

104   seroconversion showed IgG SHM frequencies comparable to HHC, there is a rapid increase in

105   the proportion of IgG-expressing (IgG+) B cells with low SHM during the DPSO (Figure 2A,

106   lower panels). Notably, prior to seroconversion, B cells expressing a few IGHV genes,

107   particularly IGHV3-30-3 and IGHV1-2, showed earlier changes than the rest of the repertoire,

108   with increased IgG class switched low-SHM clones (Figures 2C and 2D). IGHV3-9 showed a

109   similar trend but was not significant (Figures 2C and 2D).

110   We previously observed a similar influx of low mutation clones into the IgG compartment in

111   acute Ebola virus (EBOV) infection (Davis et al., 2019), but in EBOV acute viral infection there

112   was a prolonged delay (lasting months) in accumulation of SHM in those clones. In contrast,

113   examination of clones detected at two or more time points show that after the initial appearance

114   of low-SHM clones, the COVID-19 patients show increases in the proportion of IgG+ B cells

115   with intermediate SHM frequencies (2-5%) within the first three weeks post-onset of symptoms

116   in the patients for whom the longest time courses were observed (patients 7453 and 7455, Figure

117   2B). Similarly, examination of the total clones within each isotype shows the appearance of low-

118   SHM clones post-seroconversion within the first two weeks post-onset of symptoms, and

119   subsequent increases in SHM over the following two weeks (Figure 2E). In further contrast to

120   EBOV, COVID-19 primary infection stimulated polyclonal B cell responses with both IgG and,

121   in some patients, IgA subclasses, rather than IgG alone (Figure 1). Overall, among IgG+ B cells

122   in COVID-19 patients, the proportion of IgG1+ cells was increased, with decreases in IgG2 and

123   IgG3, and median usage of IgG1 was 1.7-fold greater than that seen in HHC B cells (Table S1).

124   Comparison of the IGHV genes used by COVID-19 and HHC individuals (Figure S2) revealed

125   skewing of the responding IGH repertoires away from frequently utilized IGHV genes in HHC,

126   such as IGHV3-7, IGHV3-23, and IGHV5-51, and enrichment of IGHV1-24, IGHV3-9, IGHV3-

127   13, and IGHV3-20 in IgG+ B cells. The preferential selection of B cells using particular IGHV

128   genes has been observed in other antiviral responses, such as the preference for IGHV1-69 in

129   response to some influenza virus antigens (Avnir et al., 2016). Highly utilized IGHV genes in

130   IgG-seroconverted COVID-19 patients display low median SHM in IgG1-switched B cells

131   (range 2.4-7.5%), compared to higher median IgA1 SHM (range 5.8-9.5%) (Figure 2C).

132   In the SARS-CoV-2 stimulated B cell proliferations, high-frequency expanded clones detected in

133   two or more replicate IGH sequence libraries generated from separate aliquots of template

134   showed increased proportions of low-SHM members (Figures S3A and S3B, IgG1: p-value =

135   0.005, IgG2: 0.014, IgG3: 0.036). Expanded clones also had longer and more hydrophobic IGH

136   complementarity-determining region-3 (CDR-H3) sequences in the class switched isotypes

137   compared to HHC (Figure 2F), highlighting IGHV features selected in B cells responding to

138   SARS-Cov-2 infection and consistent with a rapid proliferation of cells recently differentiated

139   from naïve B cells (Grimsholm et al., 2020). CDR-H3 charge and aromaticity showed modest

140   differences in COVID-19 patients compared to HHC, including more negative charge in non-

141   expanded clones (Figure S3C). Notably, the relative IGHV gene usage frequencies in expanded

142   clones compared to non-expanded clones of COVID-19 patients showed a different pattern than

143   overall IGHV gene usage, with IGHV1-24, IGHV3-13, and IGHV3-20 frequencies that were

144   increased in the total repertoire but used less often in expanded clones, suggesting that the B

145   cells expressing these IGHV genes are highly polyclonal with small clone sizes. Eleven IGHV

146   genes were significantly enriched in expanded clones versus non-expanded clones (Figure S3D)

147   suggesting preferential recruitment of B cells and viral epitope binding by IGH using these

148   germline IGHV segments.
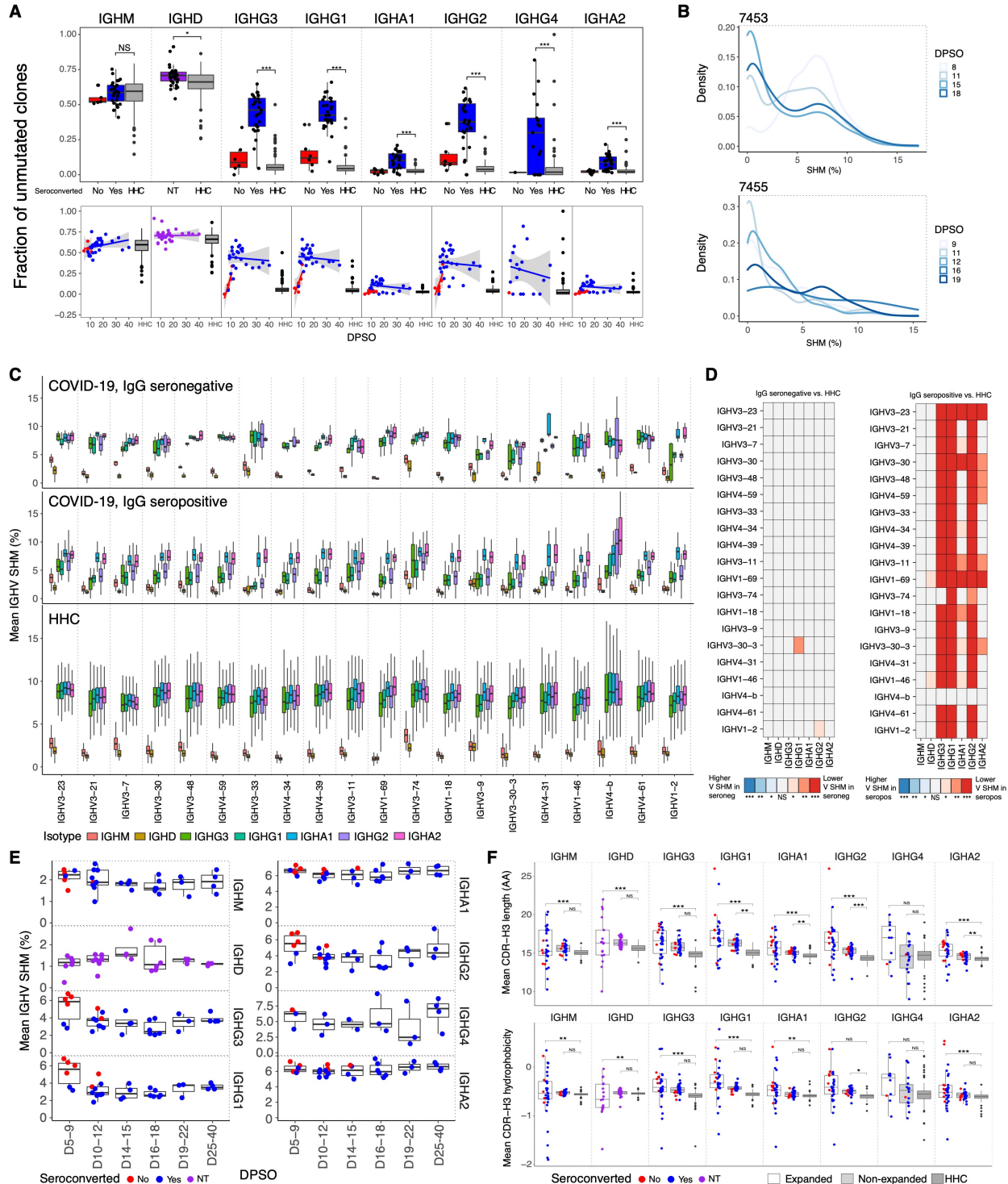
Figure 2. IGH repertoire signatures of SARS-CoV-2 infection. (A) Fraction of unmutated (<1% SHM) B cell lineages for each isotype subclass grouped by seroconversion status (top panel) or plotted by days post symptom onset (DPSO, bottom panel). Colors indicate patient sample serology: not tested (NT, purple), seronegative (red), and seropositive (blue) and are plotted specific to the isotype tested. Points are shown for all COVID-19 samples, whereas only

9

155   outliers are displayed for the 114 healthy human controls (HHCs). Differences between the
156   seropositive group and HHC was tested using two-sided Wilcoxon–Mann-Whitney (for patients
157   with more than one sample, the mean value of these was used). (B) Distribution of clone
158   percentage SHM plotted as kernel density for clones detected at multiple time points from
159   patients 7453 and 7455. Lines are colored by DPSO. (C) Mean IGHV SHM percent for each
160   isotype subclass observed for the IgG seronegative patient samples (top), IgG seropositive
161   samples (middle) or HHCs (bottom). IGHV order is based on the 20 most common IGHV genes
162   in IgM in the patients and isotypes are plotted by their chromosomal ordering. The plot axes
163   were chosen to show the box-whiskers on a readable scale; rare outlier points with extreme
164   values are not shown but were included in all analyses. (D) Heatmap of patient IGHV gene SHM
165   for seroconverted and non-seroconverted samples compared to HHC using paired Wilcoxon tests
166   with Bonferroni correction for multiple hypothesis testing. The color scale encodes the
167   significance level and whether the SHM was higher (blues) or lower (reds) in COVID-19 relative
168   to HHC. (E) Longitudinal SHM for each isotype subclass for COVID-19 patients are plotted
169   binned by DPSO. Points are colored for each sample's seroconversion status and boxplots
170   summarize median and interquartile ranges. (F) Mean CDR-H3 length (top panel) and mean
171   CDR-H3 hydrophobicity (bottom panel), COVID-19 patient samples grouped by expanded
172   clones (white) or non-expanded clones (light grey), and total clones from HHC (dark grey).
173   Differences between the expanded/non-expanded groups and HHC were tested using one-way
174   ANOVA with Tukey's HSD test. (A), (D), and (F) ***p-value < 0.001; **p-value < 0.01; *p-
175   value ≤ 0.05; NS: p-value > 0.05.
176

177   Convergent antibody rearrangements are elicited in COVID-19 patients

178   Despite the diversity of antigen-driven antibody responses, we and others have previously

179   identified patterns of highly similar, "convergent" antibodies shared by different individuals in

180   response to pathogens such as EBOV (Davis et al., 2019) or Dengue virus (Parameswaran et al.,

181   2013). Such convergent antibodies make up a small proportion of the total virus-specific B cell

182   response in each individual (Davis et al., 2019). To identify putative SARS-CoV-2-specific

183   antibody signatures, we analyzed clones with shared IGHV, IGHJ, and CDR-H3 region length,

184   and clustered the CDR-H3 sequences at 85% amino acid identity using CD-HIT (Fu et al., 2012),

185   to find clusters spanning two or more COVID-19 patients and absent from the 114 HHC

186   individuals. 1,236 convergent clusters met these criteria and showed SHM frequencies averaging

187   1.7% (range 0.5% to 5.5%). An average of 196 convergent clusters were found per patient,

188   ranging from 69 clusters in patient 7485 to 477 clusters in patient 7455. 1,171 clusters were

189   shared pairwise between two patients, 53 clusters spanned three patients, nine clusters spanned

190   four patients, and three clusters spanned five patients (Figure 3A). To assess the significance of

191   these shared convergent clones in COVID-19 patients, we undertook an analysis of 13 randomly

192   selected HHCs with the same parameters and 100 permutations. The number of convergent

193   clones shared by COVID-19 patients greatly exceeded the mean convergent clone counts from

194   the HHC subsampling (Figure 3B), consistent with antigen-driven shared selection of the

195   convergent clones identified in COVID-19 patients. To directly test the antigen specificity of

196   these convergent clones, we expressed human IgG1 monoclonal antibodies (mAbs 2A and 4A,

197   Table S2) belonging to two COVID-19 convergent antibody groups identified in two patients

198   from whom paired immunoglobulin heavy and light chain sequences were obtained from single

199   B cells using the 10x Genomics platform. mAb2A had a single nonsynonymous mutation in the

200   CDR-H2 of IGHV3-30-3 and mAb4A was fully germline and used IGHV3-15. In ELISA testing,

201   both mAbs bound the SARS-CoV-2 spike protein and spike S1 domain, but not the RBD (Figure

202   3C), establishing their antigen specificity. We further validated the robustness of detection of

203   convergent clonotypes in the COVID-19 patients, and the wide distribution of these antibody

204   types in different individuals, by identifying ten SARS-CoV-2 spike RBD-specific sequence

205   clusters shared with independent external COVID-19 patient data sets (Cao et al., 2020; Noy-

206   Porat et al., 2020; Shi et al., 2020). Nine of the thirteen COVID-19 patients (69%) in our study

207   (7450, 7452, 7454, 7455, 7480, 7483, 7484, 7485, and 7486) showed these RBD-specific

208   clonotypes, highlighting the high frequency of these shared antibodies (Figure 3D and Figure

209   S4). Notably, RBD-specific antibodies are primary candidates for virus neutralizing, potentially

210   protective antibodies in recovered patients (Ju et al., 2020; Robbiani et al., 2020a).

211   We hypothesized that in addition to sharing common RBD-binding antibody types, some

212   COVID-19 patients might also demonstrate breadth in their antibody responses and recognize

213   antigens from the distinct but related sarbecovirus, SARS-CoV that was responsible for SARS.

214   Comparison of COVID-19 patient IGH sequences to published SARS patient IGH data revealed

215   convergent SARS-CoV RBD-specific antibodies in two COVID-19 patients, 7453 and 7455

216   (Coughlin et al., 2007; Pinto et al., 2020; Robbiani et al., 2020a) (Figures 3E-3G). None of these

217   SARS-CoV-specific convergent IGH sequences were detected in the 114 HHC. To evaluate

218   whether such *in silico* IGH sequence comparisons could predict the serological responses of

219   patients, we tested the plasma samples from our 13 COVID-19 patients in ELISA assays with

220   SARS-CoV RBD antigen and detected cross-reactivity in five of the 13 patients (Figure 3H).

221   Strikingly, the two patients with the highest ELISA OD_{450} values were those who had

222   demonstrated convergent IGH sequences specific for SARS-CoV RBD. The three additional

223   COVID-19 patients who were seropositive for SARS-CoV RBD antibodies had convergent IGH

224   sequences to SARS-CoV-2 in their repertoires, suggesting that the presence of these convergent

225   antibodies could be a marker of more extensive or broadly-reactive humoral immune responses

226   in patients.
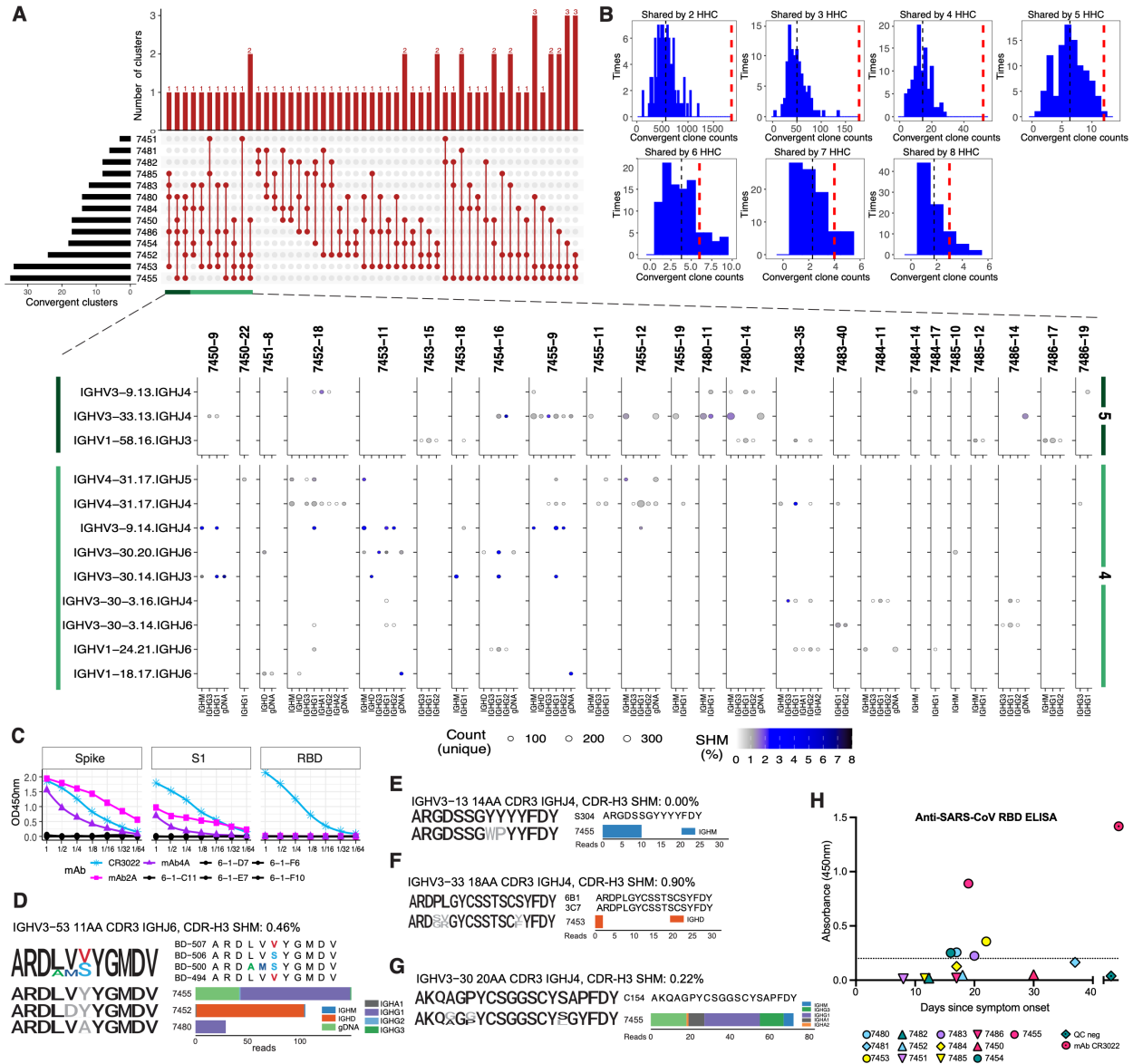
Figure 3. Convergent IGH sequences between COVID-19 patients and to reported antigen-specific IGH correlate with SARS-CoV/SARS-CoV-2 plasma cross-reactivity. (A) The distribution of convergent clusters among patient samples (top panel). The sample distribution is indicated by the lines and dots with the number of clusters sharing that sample distribution indicated by the vertical histogram bars. The total number of convergent clusters identified in each sample is indicated in the histogram to the left of the plot. (bottom panel) Lineages belonging to convergent clusters (y-axis) shared across four or five patients (columns, four-patient clusters are highlighted in light green, five-patient clusters in dark green) are plotted by the expressed isotype (x-axis). Fill color indicates the average SHM and point size shows the number of unique reads. (B) Distribution of the number of convergent clones identified in two to eight HHC subjects, determined using 100 permutations. The histogram shows the distribution of convergent clones shared by a given number of HHC samples each time. The black dashed line is the mean value, and the wide red dashed line is the number of convergent clones shared among

13

241 the same number of COVID-19 participants. (C) ELISA assay results for human IgG1 mAb
242 binding to SARS-CoV-2 spike ectodomain protein, spike S1 domain, or RBD. Negative control
243 mAbs 6-1-C11,D7,E7,F6, and F10 are overplotted in black. The SARS-CoV-2 RBD-binding
244 mAb CR3022 (ter Meulen et al., 2006; Tian et al., 2020) was used as positive control. Starting
245 concentration for mAbs was 100 ug/mL save for CR3022, which started at 0.506 ug/mL. (D-G)
246 Sequence logos of CDR-H3 AA residues from anti-SARS-CoV-2 (D, see also Figure S4) anti-
247 SARS-CoV/CoV-2 cross-neutralizing (E) or anti-SARS-CoV (F-G) convergent IGHs. For each
248 set of convergent IGH the sequence logo and alignment for the reported antigen-specific CDR-
249 H3 is shown at the top, sequence logos for clones from each patient are aligned below (colored
250 black where they match a conserved residue in the reported CDR-H3, colored for non-conserved
251 as depicted in the alignment, or gray if no match). To the side the read count per patient that
252 contributed to the sequence logo, by isotype, is graphed. The SHM frequency for the dominant
253 isotype is shown after the convergent IGH label. (H) Anti-SARS-CoV IgG ELISA detection in
254 plasma samples from COVID-19 patients. Plasma samples were analyzed for the presence of
255 anti-SARS-CoV spike RBD-binding IgG antibodies in the latest sample timepoint available for
256 each patient. A SARS-CoV-2 pre-pandemic sample pool from healthy blood donors was used as
257 a negative quality control (QC) as well as a positive control for SARS-CoV RBD (mAb
258 CR3022) (ter Meulen et al., 2006). The dotted line denotes the cut-off value for seroconversion.
259 Assays were performed in duplicate and mean OD values are shown.
260

261 **DISCUSSION**

262 In these initial months of the COVID-19 pandemic, understanding human antibody responses to

263 SARS-CoV-2 has become a global priority. Our results provide several key findings that may

264 lend some support for vaccine strategies currently under development and suggest that

265 individuals convalescent from SARS-CoV-2 infection may be, at least for some time, protected

266 against reinfection by commonly-elicited RBD-specific antibodies. The IGH repertoires of

267 patients with diagnostically confirmed SARS-CoV-2 reveal robust polyclonal responses with

268 early class switching to IgG, and to a lesser extent, IgA isotypes, and evidence of accumulating

269 SHM in responding clones within the first month after onset of symptoms, rather than the

270 delayed SHM seen in Ebola patients (Davis et al., 2019). We note that the current COVID-19

271 study and prior analysis of EBOV infection are among very few published studies of human IGH

272 repertoire longitudinal responses to primary infections; examples from acute infection with

273 Dengue virus (Appanna et al., 2016; Godoy-Lozano et al., 2016) or H5N6 avian influenza virus

14

274   (Peng et al., 2019), have either had few patients with true primary infection, or did not analyze

275   SHM development in responding B cells.

276

277   Nine of thirteen COVID-19 patients (69%) demonstrated convergent antibodies specific for the

278   viral RBD, a major target for potentially neutralizing antibodies. SARS-CoV-2 neutralizing

279   serum antibodies are reported to be present in 67-90% of patients post-infection, depending on

280   the severity of disease, neutralization assay and threshold for positive results (Robbiani et al.,

281   2020b; Suthar et al., 2020; Wu et al., 2020a). It seems reasonable to predict that vaccines based

282   on spike or RBD antigens will also stimulate B cells expressing these common antibody types in

283   a significant fraction of the human population. The response to SARS-CoV-2 infection in a

284   subset of patients also contained B cell clones expressing convergent IGH to previously

285   described SARS-CoV RBD antibodies; strikingly, the patients with these SARS-CoV-2/SARS-

286   CoV clonotypes also had the highest SARS-CoV RBD binding serum antibody IgG levels. This

287   association suggests that it may become possible to predict the fine specificity of human

288   serological responses from IGH sequence data, as the number of documented antigen-specific

289   clonotypes in public databases increases. This example also highlights the possibility that

290   common modes of human antibody response may enable some breadth of protection or humoral

291   memory against other sarbecoviruses in the future. Longitudinal tracking of IGH repertoires in

292   larger patient cohorts, further investigation into the binding properties, functional activity and

293   serum antibody levels produced by convergent responding clones in patients, and assessment of

294   clinical outcomes under conditions of exposure to infection will be important next steps toward

295   determining the immunological correlates of protection against SARS-CoV-2 infection.

296

15

ACKNOWLEDGMENTS

AUTHOR CONTRIBUTIONS

C.A.B. and S.D.B. conceived the project. A.R., A.J.R. recruited, enrolled, and consented patients and contributed to clinical sampling and processing. S.C.A.N., R.A.H., K.R., B.S., J-Y.L., A.E.P., J.N., A.R.O-C., K.E.Y., B.D. and B.A.P. performed the experiments. H.Y.C., A.T.S., T.S.J., P.S.K. and T.T.W. contributed to serological or 10x assays, and analysis. S.C.A.N., F.Y.,

319   R.A.H., K.J.L.J., K.R., and B.A.P. contributed to data analysis. S.C.A.N., F.Y., R.A.H., K.J.L.J.,

320   K.R., C.A.B., and S.D.B. wrote the manuscript. All authors edited the manuscript.

321

322   **DECLARATION OF INTERESTS**

323   A.T.S. is a scientific founder of Immunai and receives research funding from Arsenal

324   Biosciences not related to this study. The remaining authors declare that they have no competing

325   interests.

326

327

328 **Table 1. Individual COVID-19 patient sample information in days post symptom onset**
329 **(DPSO).** Seroconversion was determined by ELISA to the SARS-CoV-2 RBD antigen (STAR
330 METHODS).

Patient ID	DPSO	IgA seroconversion	IgG seroconversion	IgM seroconversion	gDNA library	cDNA library
7450	9	Yes	Yes	Yes	Yes	Yes
7450	22	Yes	Yes	Yes	Yes	Yes
7450	25	Yes	Yes	Yes	Yes	No
7450	27	Yes	Yes	Yes	Yes	Yes
7451	8	No	No	No	Yes	Yes
7452	18	Yes	Yes	Yes	Yes	Yes
7453	8	No	No	No	Yes	Yes
7453	11	No	No	No	Yes	Yes
7453	15	Yes	Yes	Yes	Yes	Yes
7453	18	Yes	Yes	Yes	Yes	Yes
7453	20	Yes	Yes	Yes	Yes	No
7454	16	Yes	Yes	Yes	Yes	Yes
7455	9	Yes	Yes	Yes	Yes	Yes
7455	11	Yes	Yes	Yes	Yes	Yes
7455	12	Yes	Yes	Yes	Yes	Yes
7455	16	Yes	Yes	Yes	Yes	Yes
7455	19	Yes	Yes	Yes	Yes	Yes
7480	11	Yes	Yes	Yes	Yes	Yes
7480	14	Yes	Yes	Yes	Yes	Yes
7480	17	Yes	Yes	Yes	Yes	No
7481	32	Yes	Yes	Yes	Yes	Yes
7481	35	Yes	Yes	Yes	Yes	No
7481	37	Yes	Yes	Yes	Yes	No
7482	5	No	No	No	Yes	Yes
7482	8	No	No	No	Yes	Yes
7482	10	No	No	Yes	Yes	Yes
7482	12	No	Yes	Yes	Yes	Yes
7483	35	Yes	Yes	Yes	Yes	Yes
7483	40	Yes	Yes	Yes	Yes	Yes
7484	11	Yes	Yes	Yes	Yes	Yes
7484	14	Yes	Yes	Yes	Yes	Yes
7484	17	Yes	Yes	Yes	Yes	Yes
7485	8	No	Yes	Yes	No	No
7485	10	Yes	Yes	Yes	Yes	Yes
7485	12	Yes	Yes	Yes	Yes	Yes
7486	14	No	Yes	Yes	Yes	Yes
7486	17	Yes	Yes	Yes	Yes	Yes
7486	19	Yes	Yes	Yes	Yes	Yes

331

CONTACT FOR REAGENT AND RESOURCE SHARING

Further information and requests for resources and reagents should be directed to the Lead

Contact, Scott D. Boyd (sboyd1@stanford.edu).

DATA AND SOFTWARE AVAILABILITY

All data is available in the main text or the extended materials. The IGH repertoire data for this

study have been deposited to SRA with accession number PRJNA628125.

EXPERIMENTAL MODELS AND SUBJECT DETAILS

Patients admitted to Stanford Hospital with signs and symptoms of COVID-19 and confirmed

SARS-CoV-2 infection by RT-qPCR of nasopharyngeal swabs were recruited. Venipuncture

blood samples were collected in K_2EDTA- or sodium heparin-coated vacutainers for peripheral

blood mononuclear cell (PBMC) isolation or serology on plasma, respectively. Recruitment of

COVID-19 patients, documentation of informed consent, collections of blood samples, and

experimental measurements were carried out with Institutional Review Board approval (IRB-

55689). The data set containing healthy adult control immunoglobulin receptor repertoires has

been described previously (Nielsen et al., 2019). In summary, healthy adults with no signs or

symptoms of acute illness or disease were recruited as volunteer blood donors at the Stanford

Blood Center. Pathogen diagnostics were performed for CMV, HIV, HCV, HBV, West Nile

19

351 virus, HTLV, TPPA (Syphilis), and *T. cruzi*. Volunteer age range was 17-87 with median and

352 mean of 52 and 49, respectively.

353

METHOD DETAILS

354

Molecular and serological testing on COVID-19 patient samples

355

356 SARS-CoV-2 infection in patients was confirmed by reverse-transcription polymerase chain

357 reaction testing of nasopharyngeal swab specimens, using the protocols described in (Corman et

358 al., 2020; Hogan et al., 2020). An enzyme-linked immunosorbent assay (ELISA) based on a

359 protocol described in (Stadlbauer et al., 2020) was performed to detect anti-SARS-CoV and anti-

360 SARS-CoV-2 spike RBD antibodies in plasma samples from COVID-19 patients. Briefly, 96-well

361 high binding plates (Thermo Fisher) were coated with either SARS-CoV or SARS-CoV-2 spike

362 RBD protein (0.1 μg per well) overnight at 4°C. After blocking plates with 3% non-fat milk in

363 PBS containing 0.1% Tween 20, plasma samples were incubated at a dilution of 1:100 and bound

364 antibodies were detected with goat anti-human IgM/HRP (Sigma: cat. A6907, 1:6'000 dilution),

365 goat anti-human IgG/HRP (Thermo Fisher: cat. 62-8420, 1:6'000 dilution), or rabbit anti-human

366 IgA/HRP (Dako: cat. P0216, 1:5'000 dilution). Assays were developed by addition of 3,3',5,5'-

367 Tetramethylbenzidine (TMB) substrate solution. After stopping the reaction with 0.16 M sulfuric

368 acid, the optical density (OD) at 450 nanometers was read using an EMax Plus microplate reader

369 (Molecular Devices). The cut-off value for seroconversion was calculated as $OD_{450} = 0.2$ for the

370 anti-SARS-CoV IgG assay and as $OD_{450} = 0.3$ for anti-SARS-CoV-2 IgM, IgG, and IgA assays

371 after analyzing SARS-CoV-2 pre-pandemic negative control samples from healthy blood donors.

372

373 **HTS of immunoglobulin heavy chain (IGH) libraries prepared from genomic DNA and**

374 **cDNA**

375 The AllPrep DNA/RNA kit (Qiagen) was used to extract genomic DNA (gDNA) and total RNA

376 from PBMCs. For each blood sample, six independent gDNA library PCRs were set up using

377 100 ng template/library (25ng/library for 7453-D0). Multiplexed primers to IGHJ and the FR1 or

378 FR2 framework regions (3 FR1 and 3 FR2 libraries), per the BIOMED-2 design were used (van

379 Dongen et al., 2003) with additional sequence representing the first part of the Illumina linkers.

380 In addition, for each sample, total RNA was reverse-transcribed to cDNA using Superscript III

381 RT (Invitrogen) with random hexamer primers (Promega). Total RNA yield varied between

382 patients and between 6 ng-100 ng was used for each of the isotype PCRs using IGHV FR1

383 primers based on the BIOMED-2 design (van Dongen et al., 2003) and isotype specific primers

384 located in the first exon of the constant region for each isotype category (IgM, IgD, IgE, IgA,

385 IgG). Primers contain additional sequence representing the first part of the Illumina linkers. The

386 different isotypes were amplified in separate reaction tubes. Eight-nucleotide barcode sequences

387 were included in the primers to indicate sample (isotype and gDNA libraries) and replicate

388 identity (gDNA libraries). Four randomized bases were included upstream of the barcodes on the

389 IGHJ primer (gDNA libraries) and constant region primer (isotype libraries) for Illumina

390 clustering. PCR was carried out with AmpliTaq Gold (Applied Biosystems) following the

391 manufacturer's instructions, and used a program of: 95°C 7 min; 35 cycles of 94°C 30 sec, 58°C

392 45 sec, 72°C 60 sec; and final extension at 72°C for 10 min. A second round of PCR using

393 Qiagen's Multiplex PCR Kit was performed to complete the Illumina sequencing adapters at the

394   5' and 3' ends of amplicons; cycling conditions were: 95°C 15 min; 12 cycles of 95°C 30 sec,

395   60°C 45 sec, 72°C 60 sec; and final extension at 72°C for 10 min. Products were subsequently

396   pooled, gel purified (Qiagen), and quantified with the Qubit fluorometer (Invitrogen). Samples

397   were sequenced on the Illumina MiSeq (PE300) using 600 cycle kits.

398

399   **Sequence quality assessment, filtering, and analysis**

400   Paired-end reads were merged using FLASH (Magoc and Salzberg, 2011), demultiplexed (100%

401   barcode match), and primer trimmed. The V, D, and J gene segments and V-D (N1), and D-J

402   (N2) junctions were identified using the IgBLAST alignment program (Ye et al., 2013). Quality

403   filtering of sequences included keeping only productive reads with a CDR-H3 region, and

404   minimum V-gene alignment score of 200. Sample cDNA or gDNA libraries with poor read

405   coverage were excluded from further analysis (Table 1). For cDNA-templated IGH reads,

406   isotypes and subclasses were called by exact matching to the constant region gene sequence

407   upstream from the primer. Clonal identities within each subject were inferred using single-

408   linkage clustering and the following definition: same IGHV and IGHJ usage (disregarding allele

409   call), equal CDR-H3 length, and minimum 90% CDR-H3 nucleotide identity. A total of

410   1,259,882 clones (per sample, mean number of clones: 33,154; median number of clones:

411   18,503) were identified. A total of 24,888,790 IGH sequences amplified from cDNA were

412   analyzed for the COVID-19 subjects (mean: 754,205 per sample; median: 650,812) and

413   68,831,446 sequences from healthy adult controls (mean: 603,785 per individual; median:

414   637,269). Each COVID-19 patient had on average 372,304 in-frame gDNA sequences and each

415   adult control had an average of 8,402 in-frame gDNA sequences.

416

417   For each clone, the median somatic mutation frequency of reads was calculated. Mean mutation

418   frequencies for all clonal lineages from a sample for each isotype were calculated from the

419   median mutation frequency within each clone, and so represent the mean of the median values.

420   Clones with <1% mutation were defined as unmutated and clones with ≥ 1% were defined as

421   being mutated. Subclass fractions were determined for each subject by dividing the number of

422   clones for a given subclass by the total number of clones for that isotype category. Expanded

423   clones within each sample were defined as clones that were present in two or more of the gDNA

424   replicate libraries. Clonal expansion in the isotype data was inferred from the gDNA data.

425   Analyses were conducted in R (Team, 2017) using base packages for statistical analysis and the

426   ggplot2 package for graphics (Wickham, 2016).

427

428   To determine convergent rearranged IGH among patients with SARS-CoV-2 infection, we

429   clustered heavy-chain sequences annotated with the same IGHV and IGHJ segment (not

430   considering alleles) and the same CDR-H3 length were clustered based on 85% CDR-H3 amino

431   acid sequence similarity using CD-HIT (Fu et al., 2012). To exclude IGH that are generally

432   shared between humans and to enrich the SARS-CoV-2-specific IGH that are likely shared

433   among the patients, clusters were selected as informative if (1) they contained at least five IGH

434   sequences from each COVID-19 patient and were present in at least two subjects; (2) no IGH

435   sequences from HHC samples (collected prior to the 2019 SARS-CoV-2 outbreak) were

436   identified in the same convergent cluster. The same selection criteria were used to determine the

437   convergent clusters between the COVID-19 samples and previously reported IGH sequences

438   specific to SARS-CoV and SARS-CoV-2. Convergent IGH sequences between the deeply

439   sequenced COVID-19 patients and 10x Genomics single B cell immune profiling on two

440   COVID-19 patients were selected for mAb expression.

441

442   **Single-cell immunoglobulin (Ig) library preparation, sequencing, and data processing**

443   Single-cell immunoglobulin libraries were prepared using the 10x Single Cell Immune Profiling

444   Solution Kit (v1.1 Chemistry), according to the manufacturer's instructions. Briefly, cells were

445   washed once with PBS + 0.04% BSA. Following reverse transcription and cell barcoding in

446   droplets, emulsions were broken and cDNA purified using Dynabeads MyOne SILANE followed

447   by PCR amplification (98°C for 45 sec; 15 cycles of 98°C for 20 sec, 67°C for 30 sec, 72°C for 1

448   min; 72°C for 1 min). For targeted Ig library construction, 2 μL of amplified cDNA was used for

449   target enrichment by PCR (Human B cell primer sets 1 and 2: 98°C for 45 sec; 6 and 8 cycles of

450   98°C for 20 sec, 67°C for 30 sec, 72°C for 1 min; 72°C for 1 min). Following Ig enrichment, up

451   to 50 ng of enriched PCR product was fragmented and end-repaired, size selected with SPRIselect

452   beads, PCR amplified with sample indexing primers (98°C for 45 sec; 9 cycles of 98°C for 20 sec,

453   54°C for 30 sec, 72°C for 20 sec; 72°C for 1 min), and size selected with SPRIselect beads.

454   Targeted single-cell Ig libraries were sequenced on an Illumina MiSeq to a minimum sequencing

455   depth of 5,000 reads/cell using the read lengths 26bp Read1, 8bp i7 Index, 91bp Read2 and reads

456   were aligned to the GRCh38 reference genome and consensus Ig annotation was performed using

457   cellranger vdj (10x Genomics, version 3.1.0).

458

459   **Identification of convergent IGH sequences for mAb expression**

460   IGH sequences from single cells with paired productive heavy and light chains were searched

461   against COVID-19 patient bulk IGH repertoires to identify convergent sequences according to

462   the following criteria: utilization of the same IGHV and IGHJ genes; same CDR-H3 lengths; and

463   CDR-H3 amino acid sequences that were within a Hamming distance cutoff of 15% of the length

464   of the CDR-H3. Two native heavy and light chain pairs, designated mAb2A and mAb4A, which

465   were found in convergent clusters characterized by low- to mid-SHM frequencies and included

466   at least one class-switched member, were selected for cloning and expression.

467

468   **mAb cloning**

469   Paired heavy and light chain sequences from 10x single cell RNA-seq datasets were synthesized

470   by IDT as gBlocks encoding full-length heavy and light chain V(D)J regions. gBlocks were

471   resuspended at 50 ng/µL and amplified with AmpliTaq Gold (Applied Biosystems) following the

472   manufacturer's instructions, using a program of: 95°C 7 min; 30 cycles of 94°C for 30 sec, 55°C

473   for 45 sec, 72°C for 60 sec; and final extension at 72°C for 10 min. Products were gel purified

474   (Qiagen) and cloned as in-frame fusions to human IgG1, IgK or IgL constant regions into the

475   pYD7 vector (National Research Council (NRC), Canada) using Gibson Assembly Master Mix

476   (NEB) for 45 minutes at 50°C. Assembled constructs were verified by Sanger sequencing.

477

478   **mAb expression and purification**

479   Constructs were transiently transfected in HEK293-EBNA1-6E cells (NRC) at a density of 1.2-

480   1.6 million cells/mL using 25 kDa linear polyethylenimine (PEI) at a 3:1 PEI:DNA ratio in

481   OptiMEM reduced serum medium (Gibco), with a heavy chain: light chain ratio of 1:1. Cells

482   were maintained in Freestyle 293 Expression Medium (Gibco) and were supplemented with

483   0.5% tryptone 24-36 hours after transfection. Cell supernatants were harvested after 96 hours and

484   filtered through 0.45-µM filters (Millipore). Antibodies were purified via HiTrap Protein A HP

25

485   columns (GE Healthcare) run at a flow rate of 0.5-1 mL/min on Äkta Start protein purification

486   system (GE Healthcare). Antibodies were eluted using 0.1M glycine pH 2, dialyzed with 3

487   changes of PBS pH 7.4 using Slide-A-Lyzer-G2 10K dialysis cassettes (Thermo Fisher), and

488   concentrated using 30,000 kDa molecular weight cutoff polyethersulfone membrane spin

489   columns (Pierce). Final concentrations of purified antibodies were quantified with Nanodrop

490   2000 (Thermo Fisher).

491

492   **ELISA testing of mAbs**

493   ELISA conditions for mAbs were as described for COVID-19 plasma samples with the

494   following modifications: two-fold serial dilutions of mAbs were tested, starting at 100 µg/mL for

495   intra-COVID-19 convergent antibodies or peanut-specific negative mAb controls, or at 0.506

496   µg/mL for mAb CR3022; plates were coated overnight with RBD (0.1 µg per well), S1 (0.1 µg

497   per well), or spike protein (0.3 µg per well); and bound mAbs were detected with rabbit anti-

498   human IgG gamma chain-specific/HRP (Agilent: cat. P0214, 1:15,000 dilution).

499

500   **SUPPLEMENTAL INFORMATION**

501   Supplemental Information includes two tables and four figures.

502

503   **REFERENCES**

504   Appanna, R., Kg, S., Xu, M.H., Toh, Y.X., Velumani, S., Carbajo, D., Lee, C.Y., Zuest, R.,
505   Balakrishnan, T., Xu, W., et al. (2016). Plasmablasts During Acute Dengue Infection Represent a
506   Small Subset of a Broader Virus-specific Memory B Cell Pool. EBioMedicine *12*, 178-188.
507   Avnir, Y., Watson, C.T., Glanville, J., Peterson, E.C., Tallarico, A.S., Bennett, A.S., Qin, K., Fu,
508   Y., Huang, C.Y., Beigel, J.H., et al. (2016). IGHV1-69 polymorphism modulates anti-influenza

509   antibody repertoires, correlates with IGHV utilization shifts and varies by ethnicity. Sci Rep *6*,
510   20842.
511   Cao, Y., Su, B., Guo, X., Sun, W., Deng, Y., Bao, L., Zhu, Q., Zhang, X., Zheng, Y., Geng, C.,
512   et al. (2020). Potent Neutralizing Antibodies against SARS-CoV-2 Identified by High-
513   Throughput Single-Cell Sequencing of Convalescent Patients' B Cells. Cell.
514   Corman, V.M., Landt, O., Kaiser, M., Molenkamp, R., Meijer, A., Chu, D.K., Bleicker, T.,
515   Brünink, S., Schneider, J., Schmidt, M.L., et al. (2020). Detection of 2019 novel coronavirus
516   (2019-nCoV) by real-time RT-PCR. Eurosurveillance *25*, 2000045.
517   Coughlin, M., Lou, G., Martinez, O., Masterman, S.K., Olsen, O.A., Moksa, A.A., Farzan, M.,
518   Babcook, J.S., and Prabhakar, B.S. (2007). Generation and characterization of human
519   monoclonal neutralizing antibodies with distinct binding and sequence features against SARS
520   coronavirus using XenoMouse. Virology *361*, 93-102.
521   Davis, C.W., Jackson, K.J.L., McElroy, A.K., Halfmann, P., Huang, J., Chennareddy, C., Piper,
522   A.E., Leung, Y., Albarino, C.G., Crozier, I., et al. (2019). Longitudinal Analysis of the Human B
523   Cell Response to Ebola Virus Infection. Cell *177*, 1566-1582 e1517.
524   Fu, L., Niu, B., Zhu, Z., Wu, S., and Li, W. (2012). CD-HIT: accelerated for clustering the next-
525   generation sequencing data. Bioinformatics *28*, 3150-3152.
526   Godoy-Lozano, E.E., Téllez-Sosa, J., Sánchez-González, G., Sámano-Sánchez, H., Aguilar-
527   Salgado, A., Salinas-Rodríguez, A., Cortina-Ceballos, B., Vivanco-Cid, H., Hernández-Flores,
528   K., Pfaff, J.M., et al. (2016). Lower IgG somatic hypermutation rates during acute dengue virus
529   infection is compatible with a germinal center-independent B cell response. Genome Medicine *8*,
530   23.
531   Grimsholm, O., Piano Mortari, E., Davydov, A.N., Shugay, M., Obraztsova, A.S., Bocci, C.,
532   Marasco, E., Marcellini, V., Aranburu, A., Farroni, C., et al. (2020). The Interplay between
533   CD27dull and CD27bright B Cells Ensures the Flexibility, Stability, and Resilience of Human B
534   Cell Memory. Cell Reports *30*, 2963-2977.e2966.
535   Hogan, C.A., Sahoo, M.K., and Pinsky, B.A. (2020). Sample Pooling as a Strategy to Detect
536   Community Transmission of SARS-CoV-2. JAMA.
537   Huang, C., Wang, Y., Li, X., Ren, L., Zhao, J., Hu, Y., Zhang, L., Fan, G., Xu, J., Gu, X., et al.
538   (2020). Clinical features of patients infected with 2019 novel coronavirus in Wuhan, China. The
539   Lancet *395*, 497-506.
540   Ju, B., Zhang, Q., Ge, J., Wang, R., Sun, J., Ge, X., Yu, J., Shan, S., Zhou, B., Song, S., et al.
541   (2020). Human neutralizing antibodies elicited by SARS-CoV-2 infection. Nature.
542   Magoc, T., and Salzberg, S.L. (2011). FLASH: fast length adjustment of short reads to improve
543   genome assemblies. Bioinformatics *27*, 2957-2963.
544   Nielsen, S.C.A., Roskin, K.M., Jackson, K.J.L., Joshi, S.A., Nejad, P., Lee, J.Y., Wagar, L.E.,
545   Pham, T.D., Hoh, R.A., Nguyen, K.D., et al. (2019). Shaping of infant B cell receptor repertoires
546   by environmental factors and infectious disease. Sci Transl Med *11*.
547   Noy-Porat, T., Makdasi, E., Alcalay, R., Mechaly, A., Levi, Y., Bercovich-Kinori, A.,
548   Zauberman, A., Tamir, H., Yahalom-Ronen, Y., Israeli, M.a., et al. (2020). Tiger team: a panel
549   of human neutralizing mAbs targeting SARS-CoV-2 spike at multiple epitopes. (bioRxiv).
550   Parameswaran, P., Liu, Y., Roskin, K.M., Jackson, K.K., Dixit, V.P., Lee, J.Y., Artiles, K.L.,
551   Zompi, S., Vargas, M.J., Simen, B.B., et al. (2013). Convergent antibody signatures in human
552   dengue. Cell Host Microbe *13*, 691-700.

553   Peiris, J.S.M., Lai, S.T., Poon, L.L.M., Guan, Y., Yam, L.Y.C., Lim, W., Nicholls, J., Yee,
554   W.K.S., Yan, W.W., Cheung, M.T., et al. (2003). Coronavirus as a possible cause of severe acute
555   respiratory syndrome. The Lancet *361*, 1319-1325.
556   Peng, W., Liu, S., Meng, J., Huang, J., Huang, J., Tang, D., and Dai, Y. (2019). Profiling the
557   TRB and IGH repertoire of patients with H5N6 Avian Influenza Virus Infection by high-
558   throughput sequencing. Scientific Reports *9*, 7429.
559   Pinto, D., Park, Y.J., Beltramello, M., Walls, A.C., Tortorici, M.A., Bianchi, S., Jaconi, S.,
560   Culap, K., Zatta, F., De Marco, A., et al. (2020). Cross-neutralization of SARS-CoV-2 by a
561   human monoclonal SARS-CoV antibody. Nature.
562   Robbiani, D.F., Gaebler, C., Muecksch, F., Lorenzi, J.C.C., Wang, Z., Cho, A., Agudelo, M.,
563   Barnes, C.O., Gazumyan, A., Finkin, S., et al. (2020a). Convergent Antibody Responses to
564   SARS-CoV-2 Infection in Convalescent Individuals. bioRxiv, 2020.2005.2013.092619.
565   Robbiani, D.F., Gaebler, C., Muecksch, F., Lorenzi, J.C.C., Wang, Z., Cho, A., Agudelo, M.,
566   Barnes, C.O., Gazumyan, A., Finkin, S., et al. (2020b). Convergent antibody responses to SARS-
567   CoV-2 in convalescent individuals. Nature.
568   Shi, R., Shan, C., Duan, X., Chen, Z., Liu, P., Song, J., Song, T., Bi, X., Han, C., Wu, L., et al.
569   (2020). A human neutralizing antibody targets the receptor binding site of SARS-CoV-2. Nature.
570   Stadlbauer, D., Amanat, F., Chromikova, V., Jiang, K., Strohmeier, S., Arunkumar, G.A., Tan,
571   J., Bhavsar, D., Capuano, C., Kirkpatrick, E., et al. (2020). SARS-CoV-2 Seroconversion in
572   Humans: A Detailed Protocol for a Serological Assay, Antigen Production, and Test Setup. Curr
573   Protoc Microbiol *57*, e100.
574   Su, S., Wong, G., Shi, W., Liu, J., Lai, A.C.K., Zhou, J., Liu, W., Bi, Y., and Gao, G.F. (2016).
575   Epidemiology, Genetic Recombination, and Pathogenesis of Coronaviruses. Trends Microbiol
576   *24*, 490-502.
577   Suthar, M.S., Zimmerman, M., Kauffman, R., Mantus, G., Linderman, S., Vanderheiden, A.,
578   Nyhoff, L., Davis, C., Adekunle, S., Affer, M., et al. (2020). Rapid generation of neutralizing
579   antibody responses in COVID-19 patients. medRxiv, 2020.2005.2003.20084442.
580   Team, R.C. (2017). R: A Language and Environment for Statistical Computing.
581   ter Meulen, J., van den Brink, E.N., Poon, L.L.M., Marissen, W.E., Leung, C.S.W., Cox, F.,
582   Cheung, C.Y., Bakker, A.Q., Bogaards, J.A., van Deventer, E., et al. (2006). Human Monoclonal
583   Antibody Combination against SARS Coronavirus: Synergy and Coverage of Escape Mutants.
584   PLOS Medicine *3*, e237.
585   Tian, X., Li, C., Huang, A., Xia, S., Lu, S., Shi, Z., Lu, L., Jiang, S., Yang, Z., Wu, Y., et al.
586   (2020). Potent binding of 2019 novel coronavirus spike protein by a SARS coronavirus-specific
587   human monoclonal antibody. Emerging Microbes & Infections *9*, 382-385.
588   van Dongen, J.J., Langerak, A.W., Bruggemann, M., Evans, P.A., Hummel, M., Lavender, F.L.,
589   Delabesse, E., Davi, F., Schuuring, E., Garcia-Sanz, R., et al. (2003). Design and standardization
590   of PCR primers and protocols for detection of clonal immunoglobulin and T-cell receptor gene
591   recombinations in suspect lymphoproliferations: report of the BIOMED-2 Concerted Action
592   BMH4-CT98-3936. Leukemia *17*, 2257-2317.
593   Wickham, H. (2016). ggplot2: Elegant Graphics for Data Analysis. (Springer-Verlag New York).
594   Wu, F., Wang, A., Liu, M., Wang, Q., Chen, J., Xia, S., Ling, Y., Zhang, Y., Xun, J., Lu, L., et
595   al. (2020a). Neutralizing antibody responses to SARS-CoV-2 in a COVID-19 recovered patient
596   cohort and their implications. medRxiv, 2020.2003.2030.20047365.

597   Wu, Y., Wang, F., Shen, C., Peng, W., Li, D., Zhao, C., Li, Z., Li, S., Bi, Y., Yang, Y., et al.
598   (2020b). A noncompeting pair of human neutralizing antibodies block COVID-19 virus binding
599   to its receptor ACE2. Science *368*, 1274.
600   Ye, J., Ma, N., Madden, T.L., and Ostell, J.M. (2013). IgBLAST: an immunoglobulin variable
601   domain sequence analysis tool. Nucleic Acids Res *41*, W34-40.
602   Zaki, A.M., van Boheemen, S., Bestebroer, T.M., Osterhaus, A.D., and Fouchier, R.A. (2012).
603   Isolation of a novel coronavirus from a man with pneumonia in Saudi Arabia. N Engl J Med *367*,
604   1814-1820.
605   Zhou, J.Q., and Kleinstein, S.H. (2019). Cutting Edge: Ig H Chains Are Sufficient to Determine
606   Most B Cell Clonal Relationships. J Immunol *203*, 1687-1692.
607   Zhu, N., Zhang, D., Wang, W., Li, X., Yang, B., Song, J., Zhao, X., Huang, B., Shi, W., Lu, R.,
608   et al. (2020). A Novel Coronavirus from Patients with Pneumonia in China, 2019. N Engl J Med
609   *382*, 727-733.
610
611